Solid Freeform Fabrication 2021: Proceedings of the 32nd Annual International Solid Freeform Fabrication Symposium – An Additive Manufacturing Conference
Reviewed Paper

IMPACT OF POROSITY TYPE ON MICROSTRUCTURE AND MECHANICAL PROPERTIES IN SELECTIVELY LASER MELTED IN718 LATTICE STRUCTURES

S. Ramachandra*, B. B. Ravichander*, B. Farhang*, A. Ganesh-Ram*, M. Hanumantha*, J. Marquez*, G. Humphrey*, N. Swails+, A. Amerinatanzi*†

*Mechanical & Aerospace Engineering, University of Texas at Arlington, Arlington, TX.
+ Math, Science, Nursing, and Public Health, University of South Carolina Lancaster, SC.
†Materials Science and Engineering, University of Texas at Arlington, Arlington, TX.

Abstract

Laser Powder Bed Fusion (LPBF), one of the most employed additive manufacturing techniques for metals, has opened new dimensions in realizing strong and weight reducing structures. In this study, Inconel 718 (IN718) unit cell designs, were fabricated through the LPBF technique and analyzed. Among the plethora of lattice structures in existence, BCC, BCC-Z, FCC, FCC-Z, Gyroid, Diamond and Schwarz structures have been selected to focus on. A relationship between the mechanical properties including yield strength, failure stress and strain, and hardness with each type of unit cell was established. Also, the effect of the possible defects on the hardness value was examined using microstructural analysis on samples. Scanning Electron Microscopy (SEM) analysis was also performed to examine the possible defects and its effect on the hardness of the as-built part. The SEM images of the grain structures indicated higher levels of isotropy in Gyroid, and Diamond samples compared to the rest of the samples which relates to the load bearing capacities of each unit cell structure. A similar trend was observed in terms of the uniformity of meltpool which can be linked with the consistency in yield characteristics. Further, Diamond and BCC-Z structures displayed high values of hardness in comparison with rest of the samples.

Keywords: Laser Powder Bed Fusion, Porous Structures, Mechanical properties, IN718, Microstructure, Vickers Hardness.

1. Introduction

The Inconel 718 (i.e., IN718), a superalloy with nickel as its base constituent, demonstrates extraordinary properties such as good impact resistance, excellent tensile and compressive strengths [1, 2]. It also possesses high corrosive resistance on account of elevated levels of nickel (estimated to be between 50 – 55 %) [3, 4]. IN718earns the classification of a superalloy due to its ability to retain the chemical, mechanical, and metallurgical properties at elevated temperatures of the range 650 to 725 degree Celsius [5]. With such excellent set of properties offered, the superalloy has been used in aerospace, automobile, and military applications [6-11].

The rapid advancements in technology have created a great necessity for light weight and complex structures. Implementing engineered porous and Triply Periodic Minimal Surface (TPMS) based structures into part designs provides a feasible opportunity to greatly reduce the weight of the parts. However, conventional modes of manufacturing limits the ability to produce these complex structures and hence Additive Manufacturing (AM) techniques can be employed to

accomplish the same [12]. Among various metal AM techniques at disposal, Laser Powder Bed Fusion (LPBF) is one of the widely used methods that can achieve fully dense metal parts with complex geometrical shapes [12-15]. Unlike conventional fabrication methods, the LPBF technique is capable of manufacturing IN718 parts with engineered porosity embedded into their design Due to the excellent weldability of IN718, complex lattice structures can be fabricated using the LPBF process.

Distinct types of porosity shapes can be implemented into the designs such as BCC, BCC-Z, FCC, FCC-Z, Honeycomb and Gyroid. The unit cell shapes tend to have a direct impact on the mechanical attributes of the fabricated parts. While some unit cell types display excellent compressive capabilities, other unit cell types may lack the compressive capability meanwhile display good hardness or tensile strength. A study conducted by Leary *et al.,* in which the lattice performance of FCC, BCC, FCC-Z, and BCC-Z was investigated under the uniaxial compression, a large collapse stress to plateau stress ratio was observed on the different models [16]. Similarly, Maskery *et al*. [17] performed uniaxial compression tests on Al-Si10-Mg BBC structures and found approximately 95% of the structure loss occurred at 9% strain rate. Also, the microstructure of the parts can be affected by the unit cell types which thereby lead to the variation in mechanical properties. To obtain the desired mechanical characteristics, it is crucial to establish a relationship between the cell types and their effect on the various mechanical properties.

Several studies have been performed to investigate the effect of porous structures on the mechanical properties. Sing *et al.* performed compressive tests on Ti_6A1_4V using different cellular structures and showed the effect of the process parameters on the mechanical properties as well as the elasticity of lattice structures [18]. It was concluded that at an increase of 50% in strain would render the structure incapable of regaining its original strength [19]. Qiu *et al*. performed a study to find how the laser power influences a diamond lattice of $AlSi_{10}Mg$ [5]. The samples were made using 150W and 400W laser powers. It was concluded that there is a linear relationship between the power and the strut diameter. In addition, they found an increase in melted powder sticking to the surface of the strut as the laser power increased [20].

Despite the aforementioned studies on the lattice structures, the effect of unit cell shapes on the mechanical properties and the microstructure have not been extensively researched. In our previous study, uniaxial compression tests were performed on IN718 porous structures to find the effect of cell shape on the mechanical properties. Also, microstructural analysis was performed to comprehend the effect of unit cell types on parameters such as yield and failure stresses. Among all the structures, FCC-Z showed the highest yield strength followed by BCC-Z. Similarly, in TPMS structures, Schwarz showed the highest yield strength but was significantly lower in comparison with the BCC-Z and FCC-Z structures. Following a similar trend, the melt pools of TPMS structures, especially in Gyroid and diamond were uniform in terms of depth and width whereas irregularities were observed in the other samples. This can be linked to the nature of their corresponding yield values. Upon observing the SEM images of the samples before and after compression tests, BCC, FCC, and Schwarz samples retained the shape of their unit cells to a recognizable extent post loading. However, maximum displacement was evident in Gyroid followed by Schwarz and the Z-strut counterparts outperformed the BCC and FCC porosity types [21].

2. Materials and methods

2.1 Materials and Fabrication

The IN718 powder used in this study was obtained from EOS (EOS GmbH, Krailling, Germany) and had the composition of Nickel (55%), Chromium (17%), Niobium (4.75%), Molybdenum (3.3%), and the remaining weight percentage consisted of aluminum, cobalt, and phosphorous. The average size of the powder particle was determined to be around 40 microns. An EOS M290 metal 3D printer (EOS GmbH, Electro Optical Systems, Krailling, Germany) equipped with a 400W Ytterbium fiber laser used the aforementioned powder for LPBF fabrication of the samples.

The part design process involved the creation of geometries for each of the BCC, BCC-Z, FCC, FCC-Z, Gyroid, Schwarz and Diamond lattice structures in the form of a cube with the dimensions 8 x 8 x 8mm. SolidWorks (Dassault Systemes, Vélizy-Villacoublay, France) was used to create the necessary CAD files. Though all the unit cells had the same dimensions of 2 x 2 x 2 mm, the TPMS structures, namely the Gyroid and Schwarz unit cell designs were conceived with the help of K3Dsurf and Materialise Magics (Materialise 2020, Belgium).

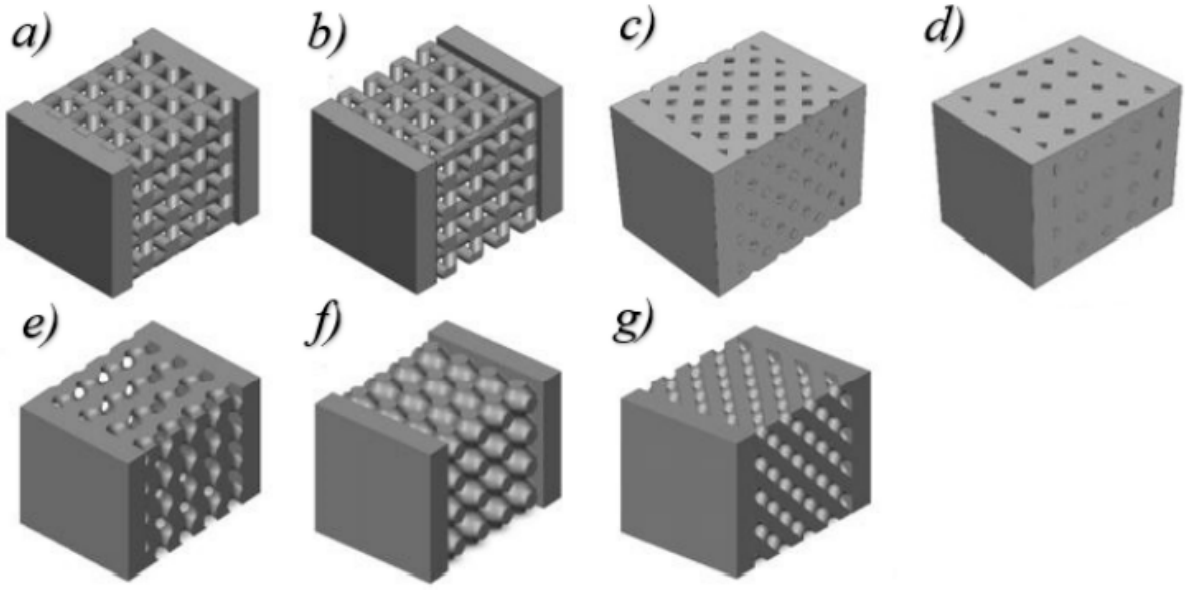

Figure 1. CAD models of a) BCC, b) BCC-Z, c) FCC, d) FCC-Z, e) Gyroid, f) Schwarz, and g) Diamond

2.2. Experiment Method

The samples were tested for hardness, mechanical properties, and microstructural analysis. The hardness values were determined on the Metal-tester model 900-391D (LECO, Missouri, USA). A Shimadzu EHF 100 fatigue testing machine was used to carry out uniaxial compression

test. The microstructural analysis involved the use of a Scanning Electron Microscope (SEM), Hitachi S-3000N Variable Pressure SEM (Hitachi, Canada).

3. Results and Discussion

3.1. Uniaxial Compression Test

Figure 1 shows the compression test results for the samples with different lattice structures [22, 23]. As can be seen in figure 1, though Gyroid and Diamond showed excellent compressive displacements of 4.836mm and 4.083mm respectively, they lacked in yield stresses. Since the maximum force used for the compression was 83KN, the overall displacement of these two specimens were not recorded to the full extent. However, this prolongation in failure can be associated to the smoothness in the transition of geometry of struts in each unit cell. The Z-variants of both BCC and FCC showed a familiar trend of outperforming their simple counterparts which can again be credited to the presence of Z-struts. Moreover, among all the samples including the TPMS structures, BCC-Z and FCC-Z attained the highest numbers in terms of compressive forces - 946MPa and 965MPa, respectively.

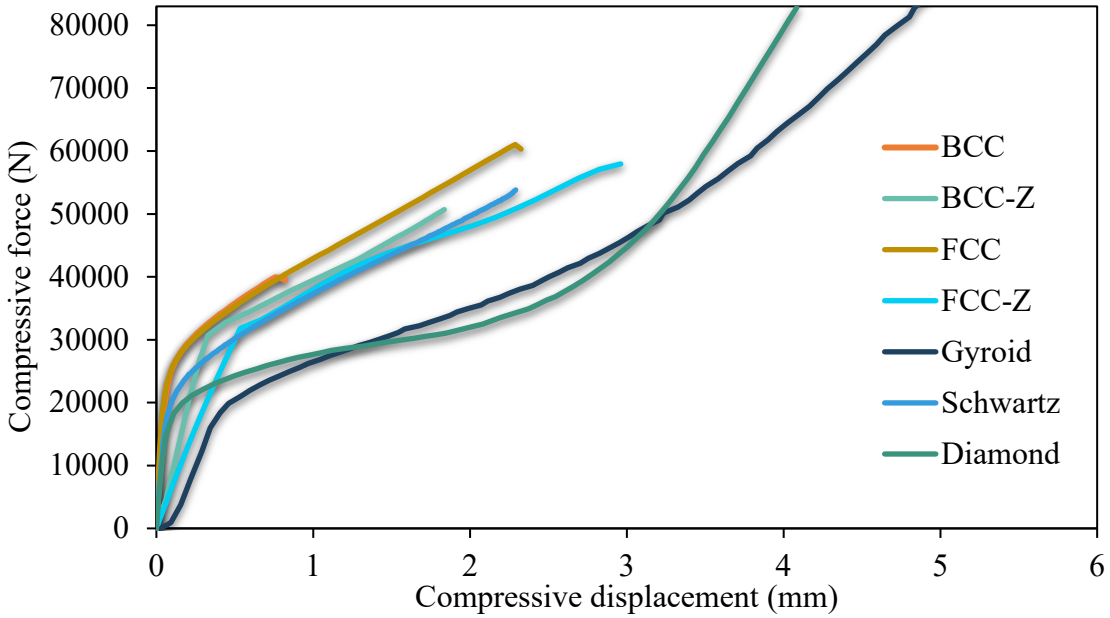

Figure 2. Compressive displacements and compressive forces sustained by each unit cell depicted graphically.

3.2. Microstructure Analysis

The Microstructural analysis was carried out using the SEM at a constant rate of magnification to reveal the nature of melt pools and the defects. According to figure 2, while samples like BCC, BCC-Z, FCC, FCC-Z, and Schwarz displayed random irregularities in the widths and depths of adjacent melt pools, Diamond and Gyroid exhibited uniform spread of melt pool sizes. This nature of variations in melt pools can be credited to the transition in the geometry of the unit cells. In the case of BCC, BCC-Z, FCC, FCC-Z and Schwarz the transition in the shape of the unit cells is instantaneous leading to a lot of variations in the melt pools. Whereas, in Gyroid

and diamond, the unit cells had a smoother geometrical transition which maintains similar and uniform development of melt pools. Uniformity in the melt pools ensures consistent and good yield results while irregularity diminishes the yield results.

Further, some of the defects observed in the SEM images involves cracks, unmelted powder, precipitates, and pores. Some of the defects can be seen enclosed in red in figure 2. Following a similar trend as the melt pools, BCC, BCC-Z, FCC, FCC-Z, and Schwarz displayed notable amounts of partially and unmelted powder on the surface and this can again be attributed to the instantaneous transition in their geometry. Conversely, the amount of partially/unmelted powder observed for the diamond and gyroid samples were negligible. While the amounts of precipitates and pores were commonly at a miniscule range in all the samples, some cracks can be observed in FCC and BCC structures. These cracks tend to initiate premature part failures making them less reliable.

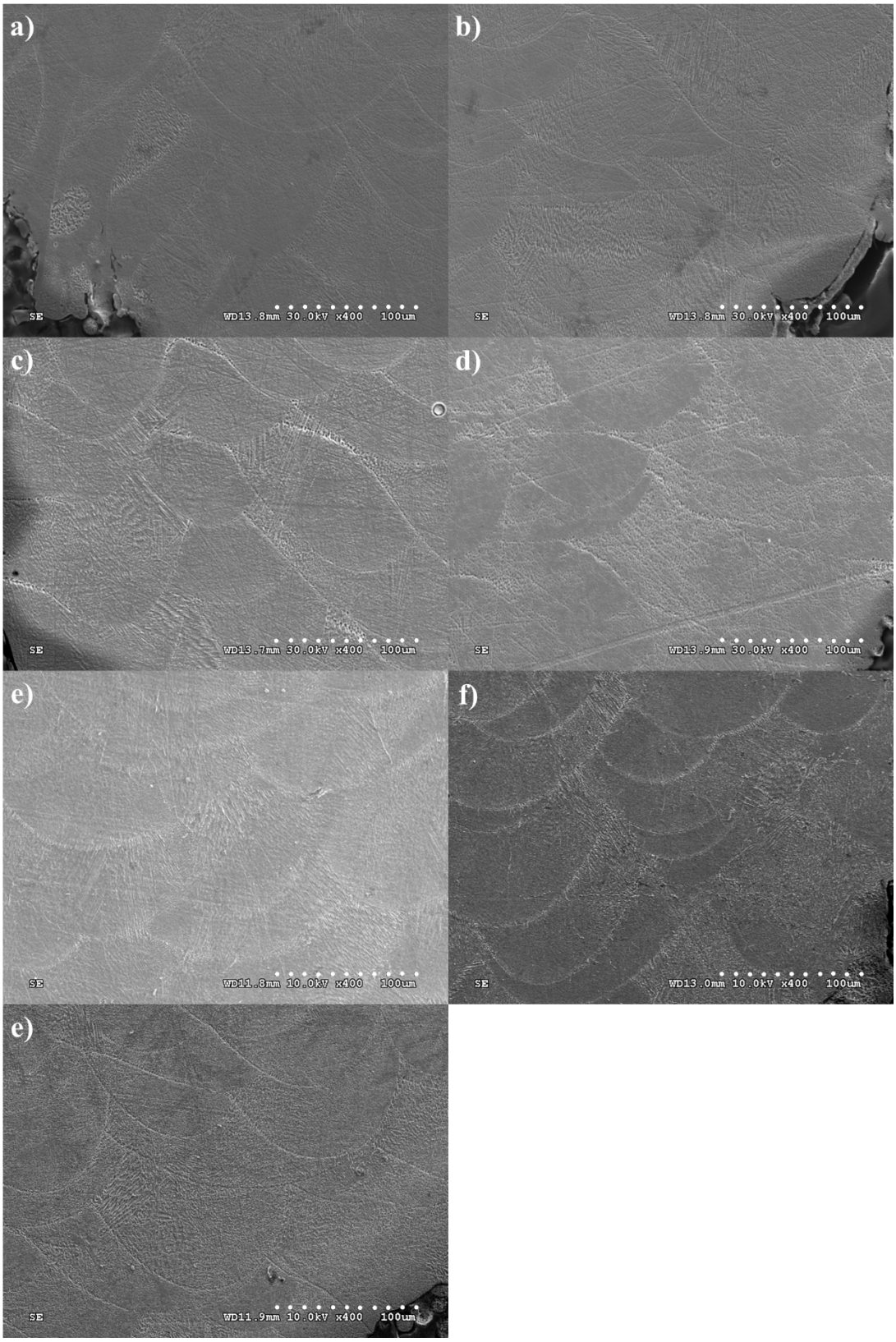

Figure 3. SEM images of Melt pools and defects observed in a) BCC, b) BCCZ, c) FCC, d) FCCZ, e) Gyroid, f) Diamond, g) Schwartz samples.

3.3. Grain Structure

The key to achieve desired mechanical attributes of a part is in the manipulation of isotropy in grain structure. SEM images of grain structure for each unit cell type can be observed below in figure 3. Samples of BCC, BCC-Z, FCC, FCC-Z and Schwarz displayed significant levels of anisotropy in grain sizes and shapes. However, Gyroid and Diamond displayed excellent isotropic grain structure. It can be noted that, because of the geometric nature of its unit cell, the Gyroid sample showed the finest quality of isotropy among all the samples. By analyzing the trends evident in the microstructural images of the grain structures, one can infer those higher levels of anisotropy can lead to early failures or reduction in the overall compressive displacement of the material.

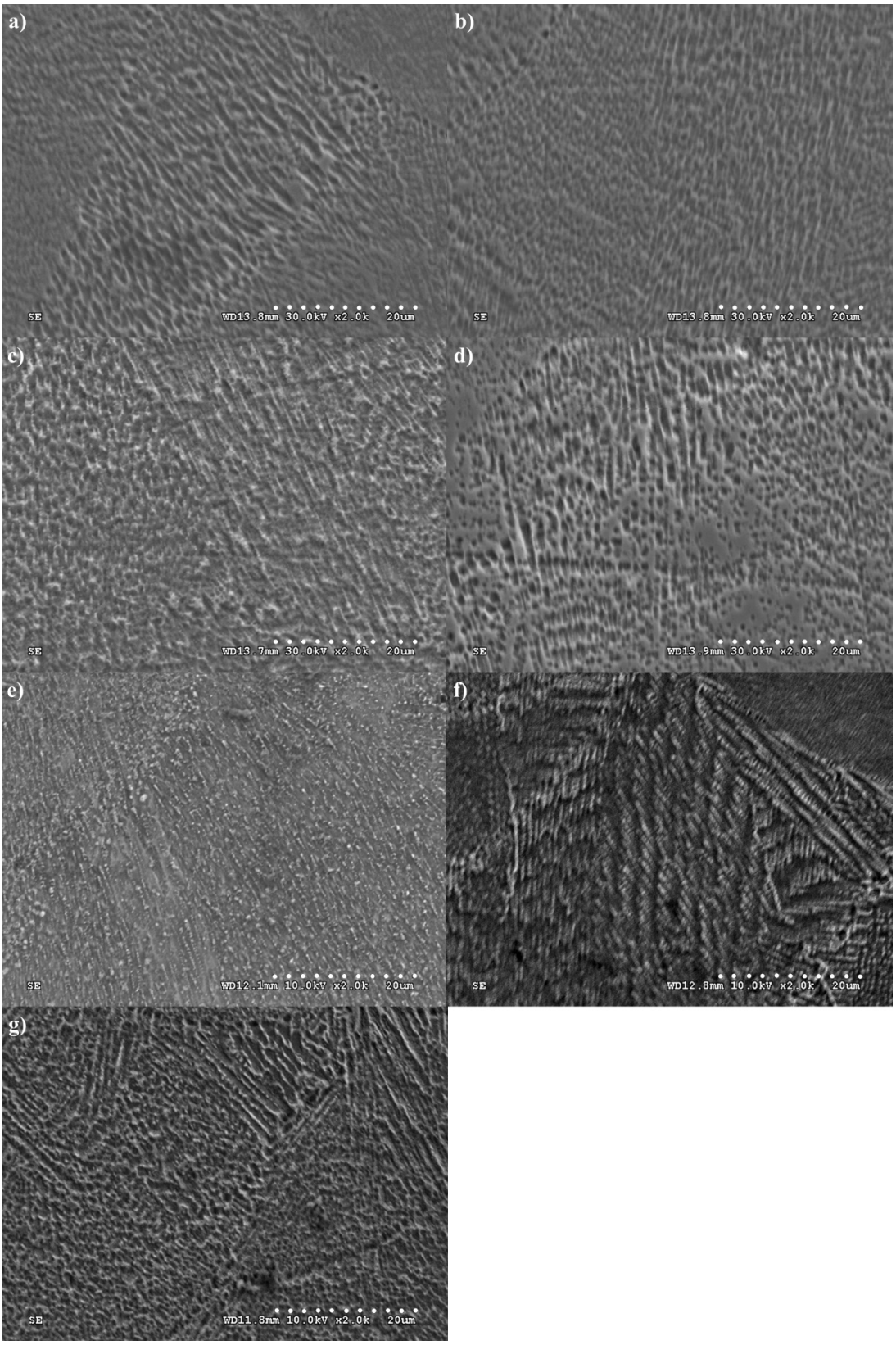

Figure 4. Grain structures of a) BCC, b) BCCZ, c) FCC, d) FCCZ, e) Gyroid, f) Diamond, g) Schwartz samples observed through SEM.

3.4. Hardness Analysis

The data (figure 4) extracted from the Vickers hardness tests revealed that the Z-strut variants of both BCC and FCC outperformed their standard counterparts. Comparing all the structures, Diamond exhibited the greatest magnitude of hardness of 421 HV and Gyroid bearing the least hardness of 337 HV. Apart from the Z-variants showing greater hardness than their simpler forms (BCC, and FCC), there is no trend evident in the variation of hardness values with respect to the unit cell shapes.

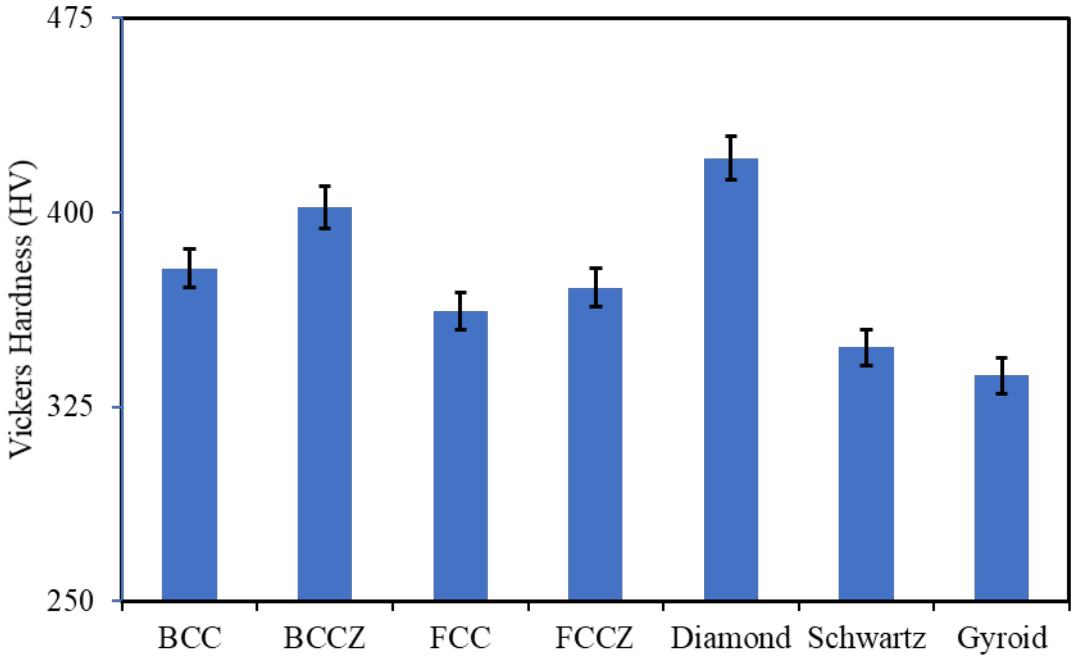

Figure 5. Vickers Hardness values of each unit cell type.

4. Conclusion

This study investigated the effect of type and shape of lattice structures on the mechanical properties, microstructure, and hardness of samples. It was revealed that unit cell geometry has a direct influence on the microstructural aspects including grain structure, defects, and melt pools successively impacting the mechanical properties of a part. It was found that unit cells with smoother transitions, displayed isotropic and defect-lacking microstructural quality, hence offering optimal mechanical properties. Additionally, a variation in the hardness value was observed among samples with different lattice types, with the highest and lowest magnitude of hardness being found for Diamond and Gyroid structures, respectively.

5. References

1. Li, J., et al., *Microstructural evolution and mechanical properties of IN718 alloy fabricated by selective laser melting following different heat treatments.* Journal of Alloys and Compounds, 2019. **772**: p. 861-870.

2. Calandri, M., et al., *Texture and Microstructural Features at Different Length Scales in Inconel 718 Produced by Selective Laser Melting. LID - 10.3390/ma12081293 [doi] LID - 1293.* (1996-1944 (Print)).
3. Wang, Z., et al., *The microstructure and mechanical properties of deposited-IN718 by selective laser melting.* Journal of alloys and compounds, 2012. **513**: p. 518-523.
4. Mortezaie, A. and M. Shamanian, *An assessment of microstructure, mechanical properties and corrosion resistance of dissimilar welds between Inconel 718 and 310S austenitic stainless steel.* International Journal of Pressure Vessels and Piping, 2014. **116**: p. 37-46.
5. Zheng, L.S., Guido & Meng, Ye & Chellali, Mohammed & Schlesiger, Ralf, *Mechanism of Intermediate Temperature Embrittlement of Ni and Ni-based Superalloys.* Critical Reviews in Solid State and Material Sciences, (2012). **37**.
6. Mostafa, A., et al., *Structure, Texture and Phases in 3D Printed IN718 Alloy Subjected to Homogenization and HIP Treatments.* Metals, 2017. **7**(6).
7. Aditya, G.-R., et al. *Study on the microstructural and hardness variations of unsupported overhangs fabricated using selective laser melting*. in *Proc.SPIE*. 2021.
8. Bharath Bhushan, R., *Correlation and effect of process parameters on the properties of inconel 718 parts fabricated by selective laser melting using response surface method*, in *Mechanical Engineering*. 2020, The University of Texas at Arlington: Arlington, TX.
9. Bharath Bhushan, R., et al. *Analysis of the deviation in properties of selective laser melted samples fabricated by varying process parameters*. in *Proc.SPIE*. 2020.
10. Ravichander, B.B., A. Amerinatanzi, and N. Shayesteh Moghaddam, *Study on the Effect of Powder-Bed Fusion Process Parameters on the Quality of as-Built IN718 Parts Using Response Surface Methodology.* Metals, 2020. **10**(9).
11. Ravichander, B.B., et al., *A Prediction Model for Additive Manufacturing of Inconel 718 Superalloy.* Applied Sciences, 2021. **11**(17).
12. Farhang, B., et al., *Study on variations of microstructure and metallurgical properties in various heat-affected zones of SLM fabricated Nickel–Titanium alloy.* Materials Science and Engineering: A, 2020. **774**: p. 138919.
13. Jia, Q. and D. Gu, *Selective laser melting additive manufacturing of Inconel 718 superalloy parts: Densification, microstructure and properties.* Journal of Alloys and Compounds, 2014. **585**: p. 713-721.
14. Bharath Bhushan, R., A. Amirhesam, and M. Narges Shayesteh. *Toward mitigating microcracks using nanopowders in laser powder bed fusion*. in *Proc.SPIE*. 2021.
15. Bharath Bhushan, R., et al. *A framework for the optimization of powder-bed fusion process*. in *Proc.SPIE*. 2021.
16. Leary, M., et al., *Selective laser melting (SLM) of AlSi12Mg lattice structures.* Materials & Design, 2016. **98**: p. 344-357.
17. Maskery, I., et al., *A mechanical property evaluation of graded density Al-Si10-Mg lattice structures manufactured by selective laser melting.* Materials Science and Engineering: A, 2016. **670**: p. 264-274.
18. Sing, S.L., F.E. Wiria, and W. Yeong, *Selective laser melting of lattice structures: A statistical approach to manufacturability and mechanical behavior.* Robotics and Computer-integrated Manufacturing, 2018. **49**: p. 170-180.
19. Maskery, I., et al., *A mechanical property evaluation of graded density Al-Si10-Mg lattice structures manufactured by selective laser melting.* Materials Science and Engineering A-structural Materials Properties Microstructure and Processing, 2016. **670**: p. 264-274.

20. Qiu, C., et al., *Influence of processing conditions on strut structure and compressive properties of cellular lattice structures fabricated by selective laser melting.* Materials Science and Engineering A-structural Materials Properties Microstructure and Processing, 2015. **628**: p. 188-197.
21. Srivathsan, S., et al., *Investigation of the strength of different porous lattice structures manufactured using selective laser melting*. SPIE Smart Structures + Nondestructive Evaluation. Vol. 11377. 2020: SPIE.
22. Srivathsan, S., *MODELING, FABRICATION, AND CHARACTERIZATION OF POROUS INCONEL 718 STRUCTURES USING SELECTIVE LASER MELTING PROCESS*, in *Mechanical and Aerospace Engineering*. 2020, The University of Texas at Arlington. p. 56.
23. Srihari, S., et al. *Investigation of the strength of different porous lattice structures manufactured using selective laser melting*. in *Proc.SPIE*. 2020.